TOWARD A WAVE DIGITAL FILTER MODEL OF THE FAIRCHILD 670 LIMITER

Peter Raffensperger

Electrical and Computer Engineering
University of Canterbury
Christchurch, New Zealand
peter.raffensperger@pg.canterbury.ac.nz

ABSTRACT

This paper presents a circuit-based, digital model of the prized 1950's vintage Fairchild® 670 vacuum tube limiter. The model uses a mixture of black boxes and wave digital filters, as a step toward a fully wave digital filter design. Wave digital filters provide an efficient, modular way to digitally simulate analog circuits. A novel model for the 6386 triode is introduced to simulate the active component in a wave digital filter model of the Fairchild 670's signal amplifier. The signal amplifier is integrated with a hybrid wave digital filter/black-box sidechain amplifier model to form a complete model of the Fairchild 670. Model test results for music and pure tones are discussed, highlighting the device's static gain characteristics and gain reduction dependent distortion. Finally, this paper discusses the model's salient features and their implications for designing dynamics processors.

1. INTRODUCTION

Vacuum tube circuits are still used in music production, long after much of the electronics industry has moved on to solid state components. Tubes have a number of advantages for audio processing, and regardless of the technical performance of some tube electronic devices, some musicians and audio engineers have come to favour their sound [1]. Rein Narma designed the Fairchild® 670[1] Stereo Limiter in the 1950's for limiting transients while mastering audio to stereo long-play phonograph records. Since then, the Fairchild 670 gained a reputation for its sound in the music production world, and there have been commercial and DIY copies as well as commercial software plug-in emulations.

Academic and commercial researchers have gone to great lengths to emulate various vacuum tube circuits for guitar [2]. None have published models of the Fairchild 670. The hardware Fairchild 670 is bulky, heavy, requires calibration and occasional replacement of hard-to-find tubes. The Fairchild 670 is also no longer manufactured; second hand units command high prices. Software emulations avoid these disadvantages. Studio engineers can use multiple software plug-in instances at once, a technique that is not possible with a single hardware unit. Furthermore, software emulation gives us an opportunity to understand the details of old designs to build on their successes.

The Fairchild 670 is a stereo limiting amplifier that controls its gain to limit the maximum absolute value of the peaks in the output signal. While clipping can reduce peaks, a limiter has less distortion because it decreases the signal amplifier gain suddenly on the detection of a peak and only gradually increases the gain afterward.

[1]Fairchild® is a registered trademark of Avid Technology, Inc., which is in no way associated or affiliated with the author.

Fig. 1 shows a block diagram of the Fairchild 670. The Fairchild 670 circuit is a feedback design as the 'sidechain' amplifier monitors the output voltage to control the gain of the signal amplifier. The user interface of the Fairchild 670 has few controls. Each of the two channels has a volume meter; 'zero' and 'balance' knobs for balancing the positive and negative going amplifier halves; a meter switch for measuring the amplifier balance; a step input attenuation knob; a continuous threshold control; and a six-way time constant select switch. There is also a control for selecting left-right or mid-side operation.

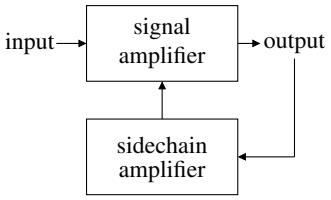

Figure 1: *An overview of the Fairchild 670 circuit. The sidechain amplifier estimates the output level which is fed back to control the gain of the signal amplifier. This non-linear amplification limits the voltage of the peaks in the output.*

Wave digital filters [3] provide an efficient way to digitally simulate analog circuits. Wave digital filters are modular at the electronic component level and are parameterised by real component values. Section 3 is a short introduction to wave digital filters. This model makes extensive use of wave digital filters to emulate subcircuits of the Fairchild 670. The intention of this line of research is to make a complete wave digital filter model of the Fairchild 670, but the present model incarnation has a mixture of black boxes and wave digital filters. As shown in Fig. 1, the model has two main parts: the sidechain amplifier, described in Section 5, which estimates the current signal level and creates a voltage signal to control the gain of the signal amplifier, described in Section 4. The sidechain amplifier model is simplified by replacing the vacuum tube amplifier with a black-box static non-linearity while the signal amplifier is modelled in detail, using a non-linear wave digital filter based on the 6386 remote cutoff vacuum triode. Section 2 describes a novel black-box model of the 6386 tube that fits the performance curves given in the General Electric datasheet.

The resulting performance of the model is detailed in Section 6 and conclusions are drawn in Section 7. This paper contributes to the wider study of digital audio effects by:

- presenting a novel model for the 6386 triode,

- applying the triode model to a wave digital filter emulation of the Fairchild 670 signal amplifier,
- and integrating a hybrid wave digital filter/black box sidechain amplifier model for a complete digital Fairchild 670 model. This model is useful for preserving and understanding past music production techniques and informing the designs of future dynamics processors.

2. 6386 REMOTE CUTOFF TRIODE MODEL

The signal amplifier of the Fairchild 670 is a 'variable-μ' Class A amplifier using the General Electric 6386 triode. The 'μ' factor of a vacuum tube is a measure of its amplification; the AC μ value for the 6386 tube depends on the DC component of the grid-cathode voltage. This unusual property is called 'remote cutoff' because the grid-cathode voltage must take an unusually large negative value to get a small anode-cathode current, as shown in Fig. 2. Existing triode models [4, 5] were designed for tubes like the 12AX7 which do not have the remote cutoff characteristic of the 6386.

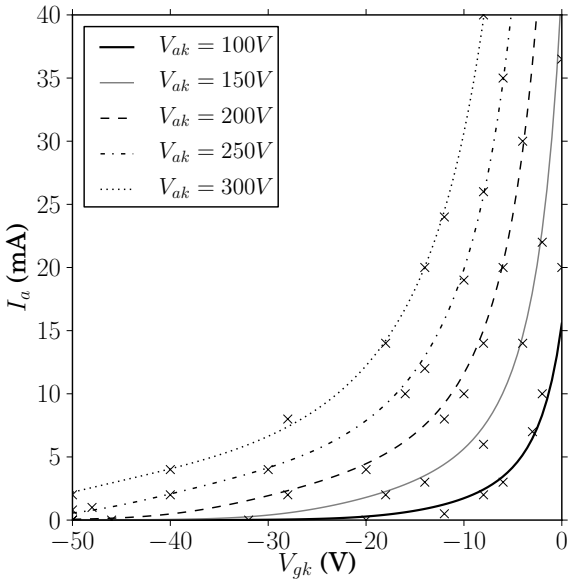

Figure 2: *The modelled 6386 triode transfer characteristics. The points used to fit the curves were taken from the datasheet [6] and are shown with x's.*

Because the remote cutoff characteristics of the 6386 tube are an essential part of the Fairchild 670, this model uses a novel black-box triode model where the anode current (in amps) is modelled as:

$$I_a = \frac{p_1 V_{ak}^{p_2}}{(p_3 - p_4 V_{gk})^{p_5} \left[p_6 + \exp\left(p_7 V_{ak} - p_8 V_{gk}\right)\right]} \tag{1}$$

where V_{gk} is the grid-cathode voltage (in volts), V_{ak} is the anode-cathode voltage (in volts) and p_1 through p_8 are parameters, with values as given in Table 1. The model parameters were calculated using Levenberg-Marquardt least squares estimation [7] and hand tuning to fit the 6386 characteristics as given in the General Electric 6386 datasheet [6]. Fig. 2 shows the transfer characteristics of the model. Because V_{gk} is negative in the Fairchild 670 circuits, the grid current is assumed to be negligible.

Table 1: *6386 remote cutoff triode model parameters for Eq. 1.*

p_1	3.981×10^{-8}
p_2	2.383
p_3	0.5
p_4	0.1

p_5	1.8
p_6	0.5
p_7	-0.03922
p_8	0.2

3. WAVE DIGITAL FILTERS

Digital filters can be designed so that one stage has no impact on the transfer function of the next stage. However, analog electronic components interact with other connected components. Consider, for example, the transformer model shown in Fig. 3. The voltage across the input termination resistor, R_{tr}, depends, for example, on the value of the load resistor, R_L. Wave digital filters provide a way to simulate analog circuits in a modular way such that the physical component values are parameters of the digital filter. The wave digital filter method is used here because its modular nature offers some advantages over other methods, such as using Kirchhoff circuit quantities for simulation. Some advantages of wave digital filters are: the circuit component values or topology can be changed in real time without restarting the circuit simulation, automatic code generation techniques can be used for rapid software prototyping and careful structuring of the component connection tree permits efficient computation of non-linear effects [8]. Wave digital filters use the bilinear z-transform to discretise the continuous-time quantities in analog circuits, which is equivalent to solving the circuit's differential equations with trapezoidal numerical integration.

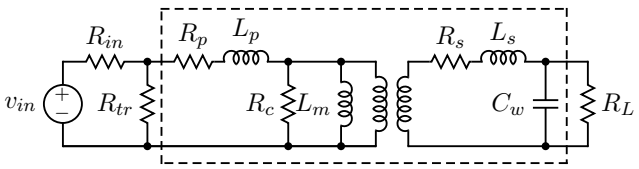

Figure 3: *A transformer model (inside the dotted box) driven by a resistive voltage source with an input termination resistor and a resistive load.*

Wave digital filter circuits are represented with block diagrams in a way similar to bond diagrams [9]. Fig. 4 shows the wave digital filter equivalent block diagram of the transformer model circuit from Fig. 3. Each individual analog component maps to an equivalent wave digital filter component where 'wave' quantities replace the Kirchhoff voltage and current:

$$a(t) = v(t) + Ri(t) \tag{2}$$

$$b(t) = v(t) - Ri(t) \tag{3}$$

where R is the 'port resistance' of the component, computed from the physical properties of the component. The two terminals of resistors, inductors, voltage sources, etc. are replaced with a single port, with an incoming wave, a, and an outgoing wave, b. The internal working of each component is some function $b(t) = F[a(t)]$,

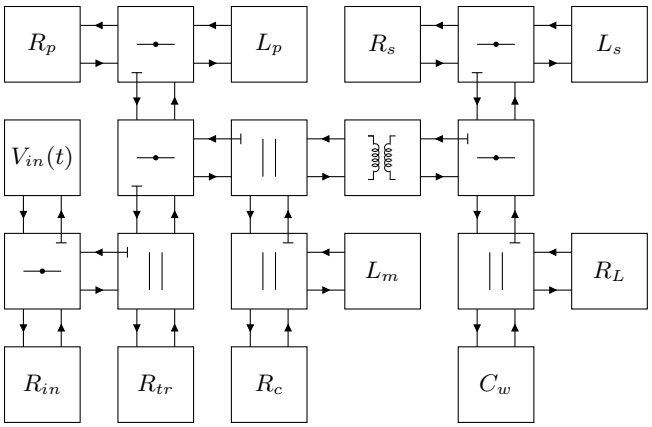

Figure 4: *A wave digital filter transformer model driven by a resistive voltage source with an input termination resistor and a resistive load. In this figure, the transformer symbol represents an ideal transformer, with its primary coil on the left and its secondary on the right.*

made up of the standard digital signal processing operations of multiplication, addition and delay by one sample. For example, a capacitor has a port resistance of $1/(2CF_s)$, where F_s is the sampling rate and C is its capacitance, and its outgoing wave is computed as $b(t) = a(t-1)$. For the exact details of each component, see [3].

The circuit topology is maintained by connecting elements together with three port 'adaptors.' Series adaptors relate their port waves by equating currents, and are represented in Fig. 4 as boxes with a single horizontal line crossing through a black dot. Likewise, parallel adaptors equate voltages, and are represented as boxes with two vertical lines. The two port box marked with a transformer symbol is a wave digital filter representation of an ideal transformer. Fig. 4 can be read as $V_{in}(t)$ in series with R_{in} in parallel with R_{tr} and the series combination of R_p, L_p and the parallel combination of…, and so on, for all the components in the circuit.

Observe that the wave digital filter structure in Fig. 4 forms a binary connected tree. Each adaptor has one port marked with a $\dashv$, this is the 'adapted' or reflection-free port. The port resistance of the adapted port is a function of the port resistances of the other two ports such that the outgoing wave of the adapted port is independent of the incoming wave of the adapted port. The adapted ports point to the trunk of the tree. (In Fig. 4, $V_{in}(t)$ is the trunk.) Because the adapted ports are reflection-free, the circuit can be simulated in two passes, as discussed by De Sanctis and Sarti [8]. In the first pass, each leaf computes its outgoing wave and port resistance, working through the tree until the trunk. Then, the trunk computes its outgoing wave based on its incoming wave and the port resistance that the rest of the circuit assigns to it. In the second pass, the incoming waves are computed, starting from the trunk and proceeding to the leaves.

For more detail on wave digital filters and the exact digital filter structures for various components, see the helpful article by Fettweis [3].

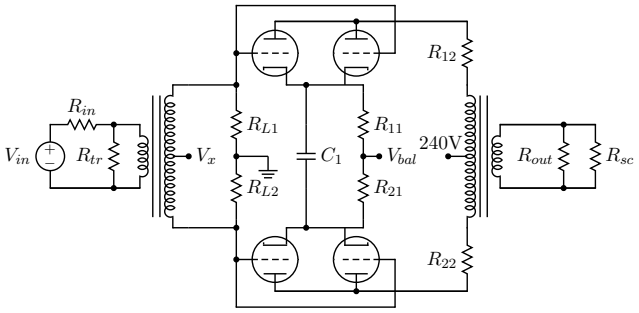

Figure 5: *A simplified circuit diagram for the Fairchild 670 signal amplifier. The triodes are 6386s.*

4. FAIRCHILD 670 SIGNAL AMPLIFIER

The Fairchild 670 limiter is a two-channel device that can act as two independent limiters for left-right stereo operation or it can separately limit the sum and difference components of the two channels (mid-side), depending on the state of a front-panel switch. The Fairchild 670's mid-side operation is called 'lateral-vertical' operation because the device was designed for cutting stereo phonographs, where the sum and difference of the stereo channels are cut as lateral and vertical grooves. For simplicity, this model considers a single channel.

Fig. 5 shows a simplified circuit diagram for one channel of the Fairchild 670 signal amplifier. The Fairchild 670 front panel includes a step attenuator to control the input level, modelled as a linear attenuation, $A_{in} \leq 1$; $A_{in} = 1$ throughout this paper. V_{in} represents the input voltage produced by whatever device is connected to the input of the Fairchild 670, after it has been attenuated by A_{in}. V_x is the output voltage of the sidechain plus a grid bias constant, modelled here as a pure voltage source, while $R_{L1} = R_{L2} = 100\,\mathrm{k}\Omega$ model both the resistive component of the sidechain and the impedance of the grids. The balance adjustment circuitry is simplified into two equivalent resistors, $R_{11} = R_{21} = 705\,\Omega$, and a constant voltage source, $V_{bal} = -3.1\,\mathrm{V}$. Because software component values have arbitrary precision and perfect stability, the studio engineer does not need to control the balancing circuit, unlike in the original hardware where R_{11}, R_{21}, and V_{bal} depend on a front panel knob position. The resistors $R_{12} = R_{22} = 33\,\Omega$ model the sensing resistors in the Fairchild 670 metering circuit. The metering circuit can measure the anode currents in either or both halves of the amplifier, but is excluded as superfluous here.

The low frequency response of the signal amplifier is determined by the bypass capacitor $C_1 = 4\,\mu\mathrm{F}$, and by the input and output transformers, which have turn ratios of $N_p/N_s = 9$ and $N_p/N_s = 1/9$, respectively. The transformers are modelled as described in Section 3, with parameters as given in Table 2, and with $R_c = 10\,\mathrm{k}\Omega$ and $L_m = 35.7\,\mathrm{H}$ for both transformers. $R_{out} = 600\,\Omega$ represents the load present by the downstream device and $R_{sc} = 1\,\mathrm{k}\Omega$ represents the input of the sidechain amplifier circuit.

The signal amplifier model has several parts. The input portion of the circuit comprises V_{in}, R_{in}, R_{tr}, V_x, R_{L1} and R_{L2}, and is used to calculate the grid voltages V_{g1} and V_{g2}. The input circuit is modelled with the wave digital filter topology in Fig. 4, using

Table 2: *Model parameters for the signal amplifier input and output transformers, and the sidechain input transformer.*

	R_p	L_p	R_s	L_s	C_w
Input	$10\,\Omega$	$4\,\text{mH}$	$50\,\Omega$	$1\,\text{mH}$	$210\,\text{pF}$
Output	$5\,\Omega$	$100\,\mu\text{H}$	$1\,\Omega$	$400\,\mu\text{H}$	$1\,\text{pF}$
Sidechain	$10\,\Omega$	$2\,\text{mH}$	$50\,\Omega$	$1\,\text{mH}$	$10\,\text{pF}$

$N_p/N_s = 1/4.5$ because only half of the output transform drives each grid. The grid voltages are calculated as:

$$V_{g1}(t) = V_{R_{L1}}(t) + V_x(t) \tag{4}$$
$$V_{g2}(t) = V_{R_{L2}}(t) + V_x(t) \tag{5}$$
$$V_{g2}(t) = -V_{R_{L1}}(t) + V_x(t) \tag{6}$$

where $V_x(t) = V_{sc}(t-1) + V_{bias}$ and $V_{sc}(t)$ is the output voltage of the sidechain and $V_{bias} = -7.2\,\text{V}$ is the bias voltage produced by the 'zero' adjust potentiometer on the front panel of the Fairchild 670. For simplicity, this model considers that V_{bias} is a constant. Because of the anti-phase nature of the input transformer, $V_{R_{L2}}(t) = -V_{R_{L1}}(t)$, and only one of $V_{R_{L1}}(t)$ or $V_{R_{L2}}(t)$ needs to be computed.

The Class A output circuit in Fig. 5 divides neatly into two parts: a 'push' half and a 'pull' half. Each half of the output stage of the signal amplifier is modelled using the wave digital filter circuit given in Fig. 6, which builds on the work of Karjalainen and Pakarinen [10, 11]. The boxes in Fig. 6 marked with both a voltage and a resistance stand for voltage sources with source resistances as marked. The box with the transformer symbol represents the transformer model given in Section 3. The complete model of the signal amplifier shown in Fig. 5 is produced by connecting the input transform circuit model to two copies of the wave digital filter structure shown in Fig. 6; the box in Fig. 6 marked '...' should be replaced with another copy of all the components in Fig. 6, except the bidirectional unit delay that is the link between the two halves of the signal amplifier.

The capacitor C_1 in Fig. 5 has to be treated with special care, because it forms an uncomputable delay-free loop [3], and because assigning it to either half of the circuit would break the symmetry of the Class A stage. This difficulty is resolved by connecting two capacitors with value $2C_1$ in series and by placing a bidirectional unit delay between the two capacitors, breaking the delay-free loop in a way that maintains the symmetry of the circuit. This way, each wave digital filter circuit has a single non-linearity, which simplifies computation. The issue of delay-free loops is discussed in more detail in Section 6.

The triode model from Section 2 is integrated into the wave digital filter circuit as in [10]. The grid voltage $V_{g1}(t)$ is computed by the input portion of the signal amplifier. The grid-cathode voltage $V_{gk1}(t)$ is approximated with the current grid voltage and the cathode voltage of the previous time step $V_{k1}(t-1)$, which is computed by the wave digital filter circuit itself. Using the delayed cathode voltage introduces errors into the circuit simulation, but errors are small because the cathode voltage changes slowly. The model from Section 2 uses Kirchhoff voltages and currents, but wave digital filters operate using incoming and outgoing waves. Consequently, the outgoing wave of the box marked 'Tube' in

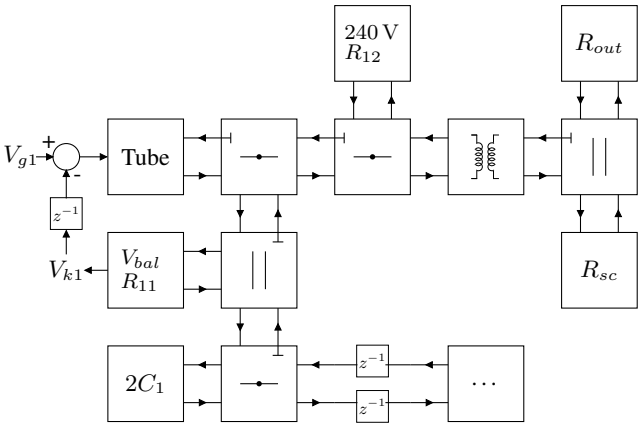

Figure 6: *A wave digital filter model of the 'push' half the output stage of the signal amplifier. In this figure, the transformer symbol represents the transformer model given in Section 3, and the box marked '...' represents the 'pull' half of the circuit, which is identical.*

Fig. 6 is computed with implicit equations:

$$V_{ak}(t) + 2R_0 I_a[V_{gk}(t), V_{ak}(t)] - a(t) = 0 \tag{7}$$
$$b(t) = V_{ak}(t) - 2R_0 I_a[V_{gk}(t), V_{ak}(t)] \tag{8}$$

where I_a is computed with Eq. 1 and R_0 is the known port resistance seen by the 'Tube' box in Fig. 6 [10]. Eq. 7 is solved using the Newton-Raphson method to compute V_{ak} which is then used to compute b in Eq. 8. The model current is multiplied by 2 because Eq. 1 represents a single 6386 triode, while the circuit has two such tubes. Consequently, the circuit can be modified to include six, eight or even more tubes at no cost, while such a change would be difficult and expensive to do in hardware.

The output voltage is computed as the difference of the push section and the pull section:

$$V_{out}(t) = V_{R_{out}}^{push}(t) - V_{R_{out}}^{pull}(t) \tag{9}$$

5. SIMPLIFIED SIDECHAIN AMPLIFIER

Fig. 7 shows an equivalent circuit diagram for the Fairchild 670 sidechain, which is modelled partially with wave digital filters and partially with a black-box static non-linearity derived from simulation results. The input transformer circuit of the sidechain amplifier is modelled as a wave digital filter circuit as in Fig. 4, with $R_{in} = 600\,\Omega$, $R_{term} = 1360\,\Omega$, $R_{load} = 152\,\text{k}\Omega$, $N_p/N_s = 1/17$, $R_c = 50\,\text{k}\Omega$, $L_m = 5.7\,\text{H}$ and with the other transformer parameters in Table 2. The value for R_{load} includes the load resistors and potentiometers in both the positive and negative halves of the sidechain amplifier inputs in Fig. 7. The output voltage for an individual potentiometer is calculated as half the voltage across R_{load}, multiplied by a voltage division ratio of the ϕ_{AC} potentiometer.

The AC and DC threshold potentiometers, ϕ_{DC} and ϕ_{AC}, jointly control the threshold, ratio and knee shape of the compression. The AC threshold is the knob marked 'threshold' on the front panel of the Fairchild 670 and the DC threshold is a screw adjust inside the box. The potentiometer ϕ_{DC} has a $100\,\text{k}\Omega$ resistance and linear taper, while ϕ_{AC} is a pair of $100\,\text{k}\Omega$ linear potentiometers with $24\,\text{k}\Omega$ resistors connected between ground and a center tap on

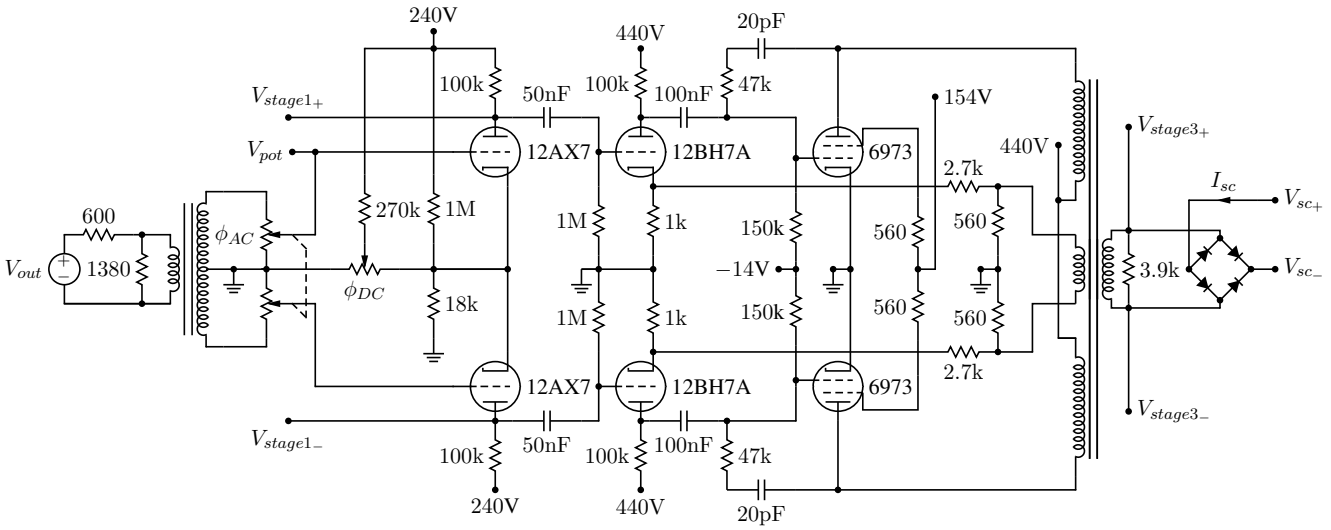

Figure 7: *A simplified circuit diagram for the Fairchild 670 sidechain.*

each potentiometer. Each AC threshold potentiometer is effectively a 76 kΩ potentiometer with a piecewise linear taper. Henceforth, for simplicity, the variables ϕ_{AC} and ϕ_{DC} represent the effective voltage division ratios of the two potentiometers.

The output transformer has four coils: a positive-going primary (the top-left coil on the right-most transformer in Fig. 7), a negative-going primary (the bottom-left coil), a secondary coil (the right coil), and a tertiary feedback coil (the middle-left coil). The turn ratios are $N_p/N_s = 4$ and $N_p/N_t = 9.5$, where N_t is the number of turns on the tertiary coil. The feedback from the tertiary coil reduces the output impedance of the amplifier. A low output impedance is essential for driving the capacitive load (shown in Fig. 8) with enough current to achieve a fast attack time. As the Fairchild 670 was originally designed as a hard limiter to prevent problems when cutting stereo phonographs, the fast attack time is an important part of the original circuit.

The sidechain amplifier is modelled as a voltage-dependent current source, with a static non-linear transfer function. A wave digital filter circuit model of the time constant circuit in Fig. 8 completes the sidechain. The component values depend on the position of a six-way switch on the front panel, with values as given in Table 3. The current source represents the sidechain amplifier model. The time constant circuit topology allows for 'program dependent release': for sustained high output levels, C_U and C_V charge, lengthening the release time when the output level decreases.

The first stage of the sidechain amplifier is a Class B amplifier with an amount of intentional crossover distortion set by the DC threshold potentiometer. The static transfer characteristic of this amplifier is approximated with a black-box mathematical model with parameters derived from simulation results. The output of this Class B stage is calculated as:

$$V_{stage1}(t) = \ln\left[\frac{1+\exp\left(V_{pot}(t)-\phi'_{DC}\right)}{1+\exp\left(-V_{pot}(t)-\phi'_{DC}\right)}\right] \qquad (10)$$

where $V_{pot} = \phi_{AC} V_{R_{load}}/2$, $V_{R_{load}}$ is calculated by the wave digital filter model of the input stage of the sidechain amplifier and

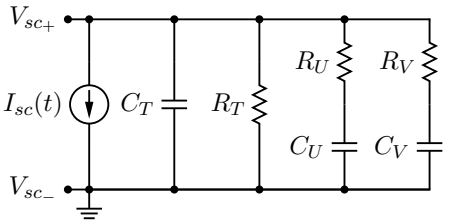

Figure 8: *The sidechain time constant circuit. The component values are different for each position of a six-way switch.*

Table 3: *The component values of the time constant circuit in Fig. 8 depend on the position of a six-way switch. R_U and R_V are open circuits for some switch positions.*

	C_T	C_U	C_V	R_T	R_U	R_V
1	2 μF	8 μF	20 μF	51.9 kΩ	open	open
2	2 μF	8 μF	20 μF	149.9 kΩ	open	open
3	4 μF	8 μF	20 μF	220 kΩ	open	open
4	8 μF	8 μF	20 μF	220 kΩ	open	open
5	4 μF	8 μF	20 μF	220 kΩ	100 kΩ	open
6	2 μF	8 μF	20 μF	220 kΩ	100 kΩ	100 kΩ

$\phi'_{DC} = 12.2(\phi_{DC} + 0.1)$. Fig. 9 shows Eq. 10 plotted against simulation results.

As with the first stage, the second and third stages of the sidechain amplifier are modelled as a black-box static non-linearity with parameters derived from circuit quantities and simulation results. The second and third stages of the sidechain amplifier form a Class A amplifier with feedback that is linear up to a point: the power supply level limits the output voltage, and the output current saturates at a maximum level. The nominal voltage gain is estimated from simulations at $A_v = 8.4$. The output voltage limitation

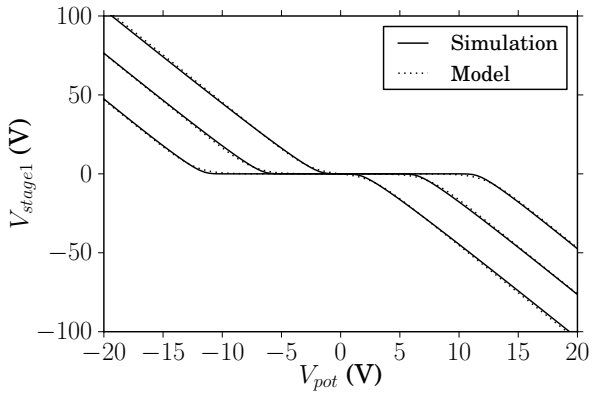

Figure 9: *Simulation results for the first stage of the sidechain amplifier, compared with the model, for* $\phi_{DC} \in \{0.1, 0.5, 0.9\}$.

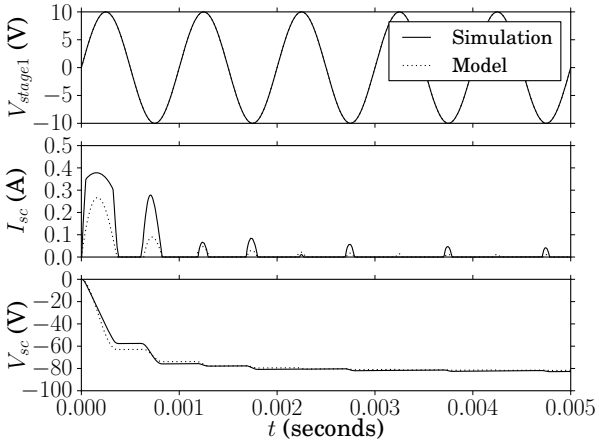

Figure 10: *Simulation results for the second and third stages of the sidechain amplifier, compared with the model.*

is modelled as a hard clip:

$$V_{stage3}(t) = \begin{cases} -100 & \text{if } A_v V_{stage1}(t) < -100 \\ 100 & \text{if } A_v V_{stage1}(t) > 100 \\ A_v V_{stage1}(t) & \text{otherwise} \end{cases} \tag{11}$$

The nominal output current through the bridge rectifier is calculated using a diode model in series with a resistance. The nominal output current, I_{nom}, against the voltage difference across the two diodes of the bridge and the resistor, V_{diff}, is calculated as an exponential transition from a line with zero slope (when the diodes are blocking) to a line with a slope dependent on the nominal output resistance (when the diodes are conducting):

$$I_{nom}(t) = \frac{2V_d}{\lambda R_{out}} \ln\left[1 + \exp\left(\frac{\lambda V_{diff}(t)}{2V_d} - \lambda\right)\right] \tag{12}$$

In Eq. 12, $\lambda = 10$ is a parameter to control the shape of the exponential transition; V_d is the nominal germanium diode drop voltage of 0.3 V; R_{out} is the nominal output resistance, estimated from simulations at $R_{out} = 160\,\Omega$ and V_{diff} is calculated as:

$$V_{diff}(t) = |V_{stage3}(t)| - \left[V_{sc_+}(t-1) - V_{sc_-}(t-1)\right] \tag{13}$$

Note that the delay-free loop inherent in the feedback topology is resolved with the unit delay in the calculation of $V_{diff}(t)$. While the fictitious delays in the signal amplifier are in parts of the circuit with low bandwidths, this delay processes full-band signals and may affect the limiter's functioning and the eventual sound quality. This issue is discussed in more depth in Section 6.

To fit simulation data, the sidechain output current with saturation is calculated as:

$$I_{sc}(t) = I_{nom}(t) - \frac{I_{max}}{10} \ln\left[1 + \exp\left(\frac{10 I_{nom}(t)}{I_{max}} - 10\right)\right] \tag{14}$$

where $I_{max} = 0.5$ A. The final sidechain output voltage, $V_{sc}(t) = V_{sc_+}(t) - V_{sc_-}(t)$, is calculated from the wave digital filter simulation of the time constant circuit in Fig. 8. Fig. 10 shows a plot of the model of Eqs. 11-14 against simulation results, for position 1 of the time constant selection switch.

6. RESULTS

Fig. 11 shows a demonstration of the model for an acoustic drum loop, processed at 44.1 kHz with 8× oversampling. The root mean squared (RMS) level relative to the peak value is higher in the processed audio than in the original, which demonstrates the limiting action of the model. Oversampling is important for accurate rendering of digital non-linearites because a non-linearity can introduce distortion products that should be higher than the Nyquist frequency. Without oversampling, those distortion products would appear as alias tones in the audible range. Yeh argues that 8× oversampling is sufficient for digital simulation of guitar distortion circuits [12]; 8× oversampling is ample here because the Fairchild 670 was not designed to produce distortion.

In addition to reducing aliasing, oversampling increases the accuracy of this model by reducing the frequency response errors inherent in bilinear z-transform discretisation and the time domain errors caused by the fictitious delays used to break the non-computable delay-free loops. Wave digital filters usually use bilinear z-transform to discretise time, resulting in a 'warped' frequency response which is less accurate at high frequencies; here this inaccuracy is mitigated by oversampling. Oversampling also plays a role in addressing the more significant difficulty of the fictitious delay added in the sidechain amplifier. By oversampling, the sidechain feedback signal changes less between each sample instant, so the errors caused by the fictitious delay are smaller. In general, breaking delay-free loops in non-linear wave digital filters with unit delays can cause instabilities and other difficulties [13]. No instabilities are present in these results, but the fictitious unit delay in the sidechain amplifier affects the model's transient limiting performance, especially for transients that have a large amount of high-frequency energy. For example, in Fig 11, the open hi-hat hit around 0.3 seconds produces a transient that is still strong in the limited model output. The unit delays added into the signal amplifier are less consequential because they are in parts of the Class A circuit that are mostly exposed to low frequencies. Some virtual analog models avoid delay-free loops entirely [14]. Quantifying the size of the errors caused by the fictitious delays

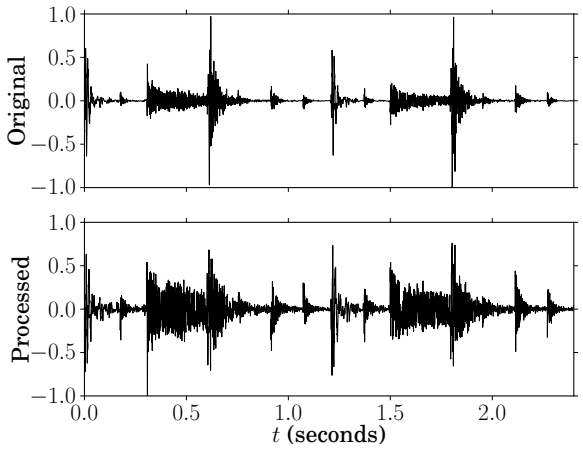

Figure 11: *The top plot shows an acoustic drum loop and the bottom plot shows the loop processed by the model, with* $\phi_{AC} = 0.5$*,* $\phi_{DC} = 0.1$*, and time constant* 1*, processed at* 44.1 kHz *with* $8\times$ *oversampling. Both plots have been normalised to the same peak value for easier visual comparison. Notice that the overall level of the processed audio is higher.*

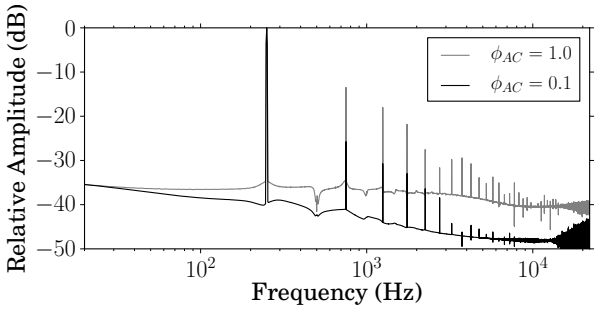

Figure 13: *Spectra of the model output driven by a* $-3.8\,\mathrm{dBm}$*,* 250 Hz *pure tone input, for two different AC threshold values, normalised for the fundamental to peak at* 0 dB*, processed at* 44.1 kHz *with* $8\times$ *oversampling. A higher AC threshold results in more gain reduction and higher distortion.*

and using techniques to eliminate their negative effects is an open area of research for this model.

Fig. 12 on p. 8 shows the static gain characteristics of the model for 1 kHz sinusoidal inputs (a), which agree in general shape to the characteristics given in the Fairchild 670 datasheet (b). Part (b) of Fig. 12 was produced by copying data from the curves in the Fairchild 670 datasheet [15]; the values of ϕ_{AC} and ϕ_{DC} were estimated from the qualitative labels in the datasheet that said, for example, 'AC THRESHOLD control slightly CW from CCW position. DC THRESHOLD control fully CW' [15]. One notable difference between the model and the specifications of the original hardware is that the gain at no limiting is higher for the model than the datasheet suggests. Perhaps this indicates that the signal amplifier input and output transformer models have less loss than the hardware transformers. For both the original hardware and the model, the AC and DC threshold controls both affect the ratio, threshold and knee shape. The Fairchild 670 manual suggests iteratively adjusting the threshold controls to get the desired gain curve. The AC threshold is directly adjustable with a knob on the front panel, while the DC threshold control is hidden under the case. Such non-standard controls may make the Fairchild 670 more difficult to use for some studio engineers, but may also increase creativity because the interface disrupts previous ways of thinking [16].

Presumably, some aspects of the 'character' of a tube audio device can be attributed to its non-linearity. Fig. 13 illustrates the non-linearity of the model; a pure tone at the input produces only odd distortion harmonics because the balanced circuit topology cancels the even harmonics. The harmonic distortion is large by modern standards. The 3rd harmonic is only 21 dB below the fundamental for $\phi_{AC} = 0.1$, and the distortion increases with higher gain reduction: the 3rd harmonic is 14 dB below the fundamental for $\phi_{AC} = 1$. However, perhaps this distortion is an important part of the Fairchild 670 sound. One speculation is that this gain-reduction-dependent distortion increases the perceived volume of the program material of the sections with more actual gain reduction, leading to less overall perceived gain reduction and hence a more 'transparent' compression.

7. CONCLUSION

This paper presents a novel black-box model for the 6386 triode and applies it to a wave digital filter model of the Fairchild 670 signal amplifier. The signal amplifier is combined with a hybrid wave digital filter/black-box sidechain amplifier model for a complete model of the Fairchild 670 limiter. The details and parameters of the model are described and model test results with music and pure tones are discussed.

Enhancements of the model presented here are possible. The model considers the power supply circuit as an ideal voltage source. While most of the amplification stages are Class A and continuously draw current from the supply, the model could be improved by considering the details of the power supply. Much of the sidechain circuit is considered as a black-box static non-linearity and could be improved by using a wave digital filter circuit; the challenge is to accurately model the feedback paths in the second and third stages without resorting to adding fictitious delays. Furthermore, the fictitious delay in the sidechain amplifier reduces the accuracy of the model. Future work on this model should also concentrate on eliminating this delay-free loop, perhaps using techniques demonstrated by Avanzini and Fontana [14].

The model was developed by studying the device schematic and with circuit simulations. This model would definitely benefit from quantitative and qualitative comparison with the original hardware; parameters could be more accurately tuned with hardware measurements and the modelling techniques could be validated by detailed listening tests.

While this paper focuses on the Fairchild 670, a number of the key ideas have more general applicability. The user interface has only a few controls, focusing the studio engineer on a particular range of sounds. There are six discrete time constant selections, rather than continuously adjustable attack and release controls, and the AC and DC threshold controls interact in unusual ways. An important part of designing an audio processor is to consider the mapping of controls to parameters and also which parameters to expose to the studio engineer. For dynamics processors specifically,

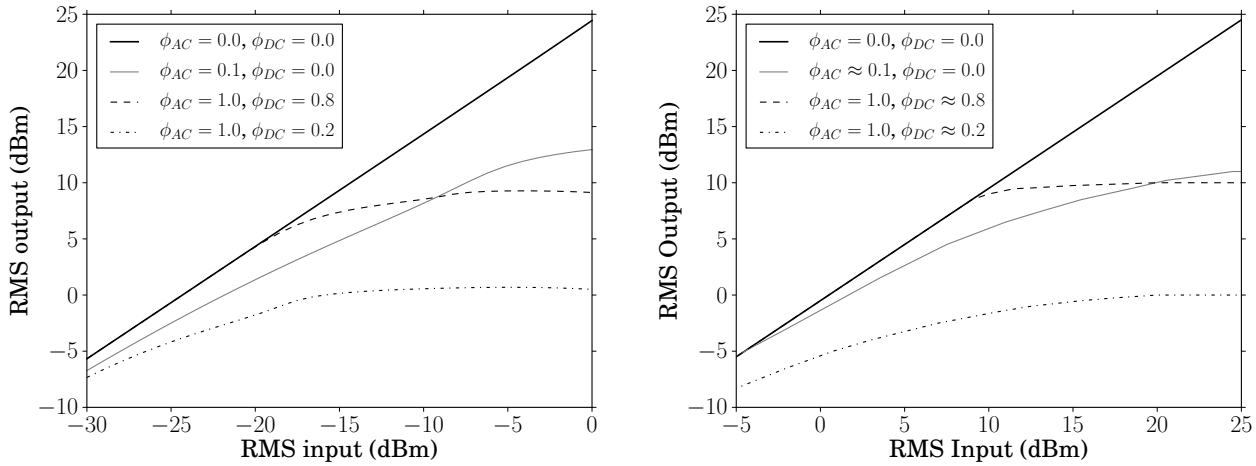

(a) Model results

(b) Curves extracted the Fairchild 670 datasheet

Figure 12: *The static gain characteristics of the Fairchild 670 model (a), at various threshold levels, and data taken from the datasheet curves [15] (b). Notice that the range of the x-axis is different for the two plots; the gain at no limiting for the model is different than that reported by the datasheet.*

the program dependent release characteristics of the time constant circuit (see Fig. 8) may be valuable in future designs. While the time constant circuit is simple, its operation can be complex. The dynamic saturation characteristics of the model suggest that future compressor designs could add an increasing amount of saturation with increasing gain reduction to crudely emulate a vintage analog processor like the Fairchild 670.

8. REFERENCES

[1] E. Barbour, "The cool sound of tubes," *Spectrum, IEEE*, vol. 35, no. 8, pp. 24–35, 1998.

[2] J. Pakarinen and D. Yeh, "A review of digital techniques for modeling vacuum-tube guitar amplifiers," *Computer Music Journal*, vol. 33, no. 2, pp. 85–100, 2009.

[3] A. Fettweis, "Wave digital filters: Theory and practice," *Proceedings of the IEEE*, vol. 74, no. 2, pp. 270–327, 1986.

[4] N. Koren, "Improved vacuum tube models for SPICE simulations," *Glass Audio*, vol. 8, no. 5, pp. 18–27, 1996.

[5] K. Dempwolf and U. Zölzer, "A physically-motivated triode model for circuit simulations," in *Proc. of the 14th Int. Conference on Digital Audio Effects (DAFx-11)*, Paris, France, 2011, pp. 257–265.

[6] "Datasheet for 6386 twin triode for Remote-Cutoff Cascode-Amplifier applications," General Electric, Electronic Components Division, Schenectady, NY, 1953.

[7] D. Marquardt, "An algorithm for least-squares estimation of nonlinear parameters," *Journal of the Society for Industrial and Applied Mathematics*, vol. 11, no. 2, pp. 431–441, 1963.

[8] G. De Sanctis and A. Sarti, "Virtual analog modeling in the Wave-Digital domain," *IEEE Transactions on Audio, Speech, and Language Processing*, vol. 18, no. 4, pp. 715 –727, 2010.

[9] J. U. Thoma, *Introduction to Bond Graphs and Their Applications*, ser. Pergamon International Library of Science, Technology, Engineering and Social Studies. Elmsford, New York, USA: Pergamon Press Inc., 1975.

[10] M. Karjalainen and J. Pakarinen, "Wave digital simulation of a vacuum-tube amplifier," in *IEEE International Conference on Acoustics, Speech and Signal Processing, 2006. ICASSP 2006 Proceedings.*, vol. 5, 2006, pp. 153–156.

[11] J. Pakarinen and M. Karjalainen, "Enhanced wave digital triode model for real-time tube amplifier emulation," *IEEE Transactions on Audio, Speech, and Language Processing*, vol. 18, no. 4, pp. 738 –746, 2010.

[12] D. T. Yeh, "Digital implementation of musical distortion circuits by analysis and simulation," Ph.D. dissertation, Stanford University, 2009.

[13] J. Pakarinen, M. Tikander, and M. Karjalainen, "Wave digital modeling of the output chain of a vacuum-tube amplifier," in *Proc. of the 12th Int. Conference on Digital Audio Effects (DAFx-09)*, 2009, pp. 55–59.

[14] F. Avanzini and F. Fontana, "Exact discrete-time realization of a Dolby B encoding/decoding architecture," in *Proc. of the 9th Int. Conference on Digital Audio Effects (DAFx-06)*, 2006, pp. 297–302.

[15] "Model 670 stereo limiter instruction manual," Fairchild Recording Equipment Corporation, Long Island City, NY, 1959.

[16] E. De Bono, *Lateral Thinking: A Textbook of Creativity*, ser. Pelican books. Harmondsworth, UK: Penguin, 1977.